Are the input parameters of integrate-and-fire neurons uniquely determined by rate and CV?

Rafael D. Vilela and Benjamin Lindner[1]

[1]*Max-Planck-Institut für Physik Komplexer Systeme, Nöthnitzer Str. 38 01187 Dresden, Germany*
(Dated: June 16, 2008)

Integrate-and-fire (IF) neurons have found widespread applications in computational neuroscience. Particularly important are stochastic versions of these models where the driving consists of a mean input (base current μ) and a fluctuating current (white Gaussian noise of intensity D). Different IF models have been proposed, the firing statistics of which depends nontrivially on the input parameters μ and D. Comparison of these models among each other or with real neurons should be performed at parameters that yield similar basic firing statistics as, for instance, the firing rate and the coefficient of variation (CV) of the interspike interval. However, it is not clear *a priori* whether for a given firing rate and CV, there is only one unique choice of input parameters for the respective model. Here we review the dependence of rate and CV on input parameters for the perfect, leaky, and quadratic IF neuron models and show analytically that indeed in all three models the firing rate and the CV of the interspike interval distribution uniquely determine the input parameters. For the leaky and quadratic IF models, we use properties of the contour lines for fixed rate and CV and also give simple numerical algorithms leading from given rate and CV to the actual input parameters.

I. INTRODUCTION

A important class of simplified neuronal models comprises integrate-and-fire neurons [1, 2] the dynamics of which can - in particular in stochastic versions - explain a number of interesting phenomena. New types of IF models are still introduced nowadays that mimic certain aspects more faithfully than other IF models do, for instance, the two dimensional resonate-and-fire model [3], IF models with adaptation currents [4], and models with specific nonlinearities [5] and relative refractory period [6, 7]. Three meanwile classic variants are the random walk model by Gerstein and Mandelbrot [8] usually referred to as the perfect IF neuron, the leaky IF model studied by Stein [9, 10], Johannesma [11], and many others (see reviews [1, 2]), and the type I normal form with noise addressed by Gutkin and Ermentrout [12] and Lindner et al. [13] also known as quadratic IF model.

It is known that the firing statistics of the various IF models as well as their response to periodic stimulation differ due to the different nonlinearities in these models. Additionally, the same numerical values of mean current μ and the intensity of the white noise D have different effect on the firing statistics of the respective models. Thus, it is not simple to compare these models among each other nor is it straightforward to compare them to experimental data [14].

One simple way of comparison is to fix a certain basic firing statistics as, for instance, the firing rate and then compare the remaining statistics as, for instance, the power spectrum of the spike train between different IF models. It is obvious that the firing rate alone is not sufficient to determine the unknown parameters (μ, D) and that also the degree of irregularity of spiking as characterized by the coefficient of variation (CV) of the interspike interval will affect the correct choice of μ, D; thus a natural choice to fix the parameters of the IF model is to prescribe rate and CV of the output spike train. However, given both statistics, it is not clear at all whether the parameters μ and D of a certain model will be uniquely determined, i.e. whether at most one parameter set (μ and D) exists for which the considered IF model generates a spike train with the desired firing statistics (rate and CV). This problem is also related to the problem of finding optimal fitting parameters for an IF model given experimental data and has been subject of several studies (see [14] and references therein). In one approach, the model parameters are inferred from subthreshold membrane measurements (for a recent reference see [15]). In another approach, model parameters must be inferred solely from interspike interval (ISI) statistics [16–19]. Most of these studies consider the leaky IF model. To the best of our knowledge, the problem of the uniqueness of input parameters has not been addressed in these or other works.

The aim of our paper is to address the question of uniqueness of input parameters for the perfect (PIF), leaky (LIF), and quadratic (QIF) IF neuron models. In spite of its apparent simplicity, this question is nontrivial since, for instance the CV may depend in a nonmonotonic way on the input parameters and so it is not clear whether the mapping of μ and D on rate and CV is invertible or not.

Here we show that rate and CV uniquely determine the input parameters for the three models. We first review the properties of rate and CV as functions of μ and D using known expressions for these statistics as functions of the model parameters and scaling relations. For the PIF, the expressions for the ISI's moments turn out to be sufficiently simple as to admit straightforward inversion. For LIF and QIF, such analytical mappings unfortunately do not exist, due to the complexity of the corresponding expressions for the moments of the ISI. In these cases, we use the properties of the contour lines for rate and CV. We show that each contour line for the rate intersects at most once each contour line for the CV. As a byproduct of this study, we present simple numerical algorithms that permit a fast calculation of the model parameters corresponding to a given rate and CV, provided that the internal parameters (membrane time constant, threshold and reset voltage values) are already known.

II. INTEGRATE-AND-FIRE NEURON MODELS

A. Definition of the models and relation to the first passage time problem

The IF models considered here consist of two ingredients: (i) a one dimensional stochastic ordinary differential equation describing the subthreshold time evolution of a variable v and (ii) a fire-and-reset rule.

The equation accounting for the subthreshold dynamics of v can be cast, for all the models considered here, as:

$$\tau \dot{v} = f_{\mathrm{model}}(v) + \mu + \sqrt{2D\tau}\xi(t), \tag{1}$$

where τ is the membrane time constant, $f_{\mathrm{model}}(v)$ is a deterministic model-specific function and ξ is Gaussian white noise with zero average and $\langle \xi(t)\xi(t')\rangle = \delta(t - t')$. Eq. (1) is in general a nonlinear Langevin equation with a white noise input (synaptic current) with mean μ and noise intensity D. Throughout this paper we measure time in units of τ, which is realized by setting $\tau = 1$.

The model-specific functions, the possible ranges for the mean input μ, and the reset and threshold values are given by:

$$f_{\mathrm{PIF}} = 0, \qquad \mu > 0, \qquad v_{th} = 1, \qquad v_r = 0, \tag{2}$$

$$f_{\mathrm{LIF}} = -v, \qquad \mu \in (-\infty, \infty), \qquad v_{th} = 1, \qquad v_r = 0, \tag{3}$$

and

$$f_{\mathrm{QIF}} = v^2, \qquad \mu \in (-\infty, \infty), \qquad v_{th} = \infty, \qquad v_r = -\infty. \tag{4}$$

The fire-and-reset rule can be expressed as

$$v(t) = v_{th} \implies \text{ spike at time } t \text{ and } v \to v_r, \tag{5}$$

i.e., whenever v reaches a threshold value v_{th} the neuron fires a spike and there is a reset of its membrane potential to a value v_r.

In the cases of PIF and LIF, the variable v can be always rescaled such that reset and threshold values are at zero and unity without loss of generality (v is then measured in units of the difference between threshold and reset); for better applicability of our results, we will keep v_r and v_{th} in all resulting formulas and equations. For the QIF, reset and threshold are at minus and plus infinity. In this case v is not interpreted as the membrane potential. Instead, Eq. (1) then corresponds to the normal form of a type I neuron [20], i.e., a neuron close to a saddle-node bifurcation.

The IF neuron model, Eqs. (5) and (1), can be alternatively interpreted as describing a Brownian particle of position v undergoing overdamped motion in a potential U_{model} such that

$$-\frac{dU_{\mathrm{model}}}{dv} = f_{\mathrm{model}} + \mu. \tag{6}$$
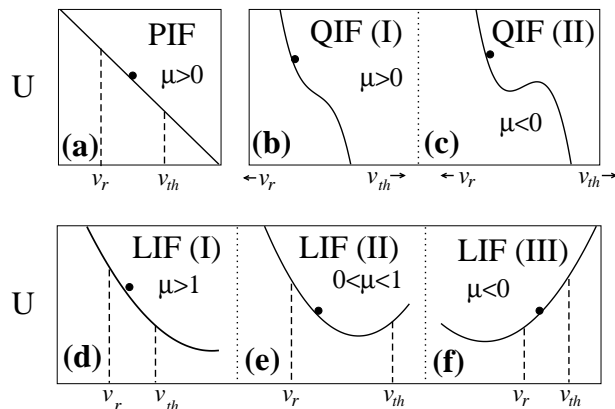
FIG. 1: Potentials for the different models (cf. Eq. (6)). The PIF is only defined in the tonic firing regime ($\mu > 0$). The QIF can be in the tonic (I) and noise-induced (II) firing regimes. The LIF occurs in the tonic (I) and noise-induced (II-III) firing regimes. The noise-induced regimes for this model can display v_r at smaller (II) or larger (III) values than the voltage value at which U attains its minimum.

In this analogy, the interspike interval of the respective neuron model turns into the first-passage time of the Brownian particle starting at the reset point towards the threshold point. Depending on the model and, in particular, on the value of μ, the passage can occur already without noise (*tonic* firing regime) or must be assisted by fluctuations (*noise-induced* firing regime). The tonic regime can be most easily illustrated in case of the PIF where the particle just slides down an inclined plane from reset to threshold (see Fig. 1a) , whereas noise is needed to reach the threshold whenever there is a barrier present between reset and threshold (QIF for $\mu < 0$, see Fig. 1c) or right at the threshold (LIF, $\mu < 1$, see Figs. 1(e) and (f)). Note that the parameter μ has different meaning in the three models. In the PIF it attains only positive values and sets merely the time scale of the system. In the QIF it is a bifurcation parameter: at negative μ the potential attains one minimum whereas for positive μ the potential is a nonlinear but monotonic function. In the LIF, the bifurcation from tonic to noise-induced firing takes place at $\mu = 1$. As we will see, for the firing statistics of the LIF it is furthermore useful to distinguish the case where $\mu < 0$: here a strong noise is required to make the neuron fire and the firing statistics shows some specific features (see below).

B.   Measures

The spike train is defined as a sum of delta functions at the spiking times, i.e., the time instants when the voltage reaches the threshold and the fire-and-reset rule is applied (cf. Fig. 2):

$$y(t) = \sum_j \delta(t - t_j). \tag{7}$$

In Eq. (7), t_j stands for the instant when the j-th spike is triggered. Fig. 2 depicts the time evolution of the subthreshold voltage as described by one of the models we address and the corresponding spike train. The time intervals $T_j = t_j - t_{j-1}$ between two immediately subsequent spikes are precisely the interspike intervals.
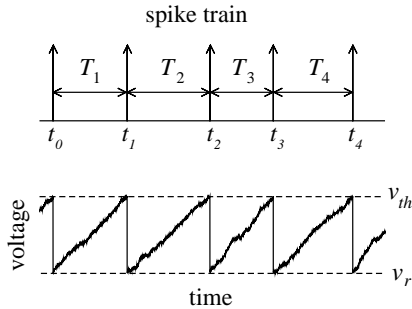
FIG. 2: Subthreshold voltage dynamics and corresponding spike train as from a simulation of Eqs. (1) and (2) (PIF) with parameters $\mu = 0.9$ and $D = 0.006$.

The spike trains considered here are stationary stochastic point processes. The *firing rate* r of such a process can be defined in three different ways: as (i) the instantaneous ensemble average of the output; (ii) the number of spikes $N(T)$ in a large time interval $(0, T)$ divided by this time window T; and (iii) the inverse mean interspike interval, i.e. we have

$$r = \langle y \rangle = \lim_{T \to \infty} \frac{N(T)}{T} = \frac{1}{\langle T \rangle}, \tag{8}$$

The *coefficient of variation* (*CV*) of the ISI is defined as:

$$CV = \frac{\sqrt{\langle \Delta T^2 \rangle}}{\langle T \rangle}, \tag{9}$$

where $\langle \Delta T^2 \rangle = \langle T^2 \rangle - \langle T \rangle^2$ is the variance of the ISI distribution. The CV can be regarded as the relative standard deviation of the ISI. For later comparison, a perfectly periodic spike train would have zero CV while a Poissonian spike train possesses a CV of one.

C.   General form of the differential equations governing the contour lines

Analytical formulas for the moments $\langle T^n \rangle$ of the first passage time in an arbitrary potential were derived by Pontryagin et al. [21]. Simplifications of these quadrature formulas as well as sum formulas for specific cases have

been put forward by many authors (for a selection, see, for instance, [1, 13, 22–27]). The first two moments determine the rate and CV, according to Eqs. (8) and (9).

In this paper we will study the rate and CV of the three models as functions of the input parameters, μ and D. In particular, we are interested in the curves for which $F(D, \mu) = \text{const}$ (F denotes either r or CV), i.e., the contour lines of the surfaces $F(D, \mu)$ over the (D, μ) parameter plane. Elementary arguments yield differential equations for functions $\mu_F(D)$ or $D_F(\mu)$ that parametrize the contour lines:

$$\frac{d\mu_F}{dD} = -\frac{\partial F/\partial D}{\partial F/\partial \mu}, \tag{10}$$

$$\frac{dD_F}{d\mu} = -\frac{\partial F/\partial \mu}{\partial F/\partial D}, \tag{11}$$

where $F \in \{r, CV\}$, provided that $\partial F/\partial \mu \neq 0$ and $\partial F/\partial D \neq 0$, respectively. We note that these conditions are not necessarily satisfied in the whole (D, μ) parameter space of the models we address. For instance, for the PIF we have in fact $\partial r/\partial D = 0$ for all valid pair (D, μ). However, for the three models studied here, at any point (D, μ) of parameter space at least one of these conditions is satisfied.

If for any pair (r, CV) the respective contour lines $\mu_r(D)$ and $\mu_{CV}(D)$ intersect at most once, then rate and CV determine uniquely the parameters of the respective integrate-and-fire model. In the following sections we will show that this is indeed the case for the PIF, LIF, and QIF.

III. PERFECT INTEGRATE-AND-FIRE NEURON

The mean and variance of the ISI are given by [23, 25]:

$$\langle T \rangle = \frac{v_{th} - v_r}{\mu}, \qquad \langle \Delta T^2 \rangle = \frac{2D(v_{th} - v_r)}{\mu^3}. \tag{12}$$

We stress that $\mu > 0$ for the PIF. For this model the expressions for rate and CV are quite simple:

$$r = \frac{\mu}{v_{th} - v_r}, \qquad CV^2 = \frac{2D}{\mu(v_{th} - v_r)}. \tag{13}$$

Moreover, the contour lines for the rate and the CV can be explicitly calculated (without resorting to the differential equations Eq. (10) and Eq. (11)):

$$\mu_{r_0}(D) = r_0(v_{th} - v_r), \qquad \mu_{CV_0}(D) = \frac{2D}{(v_{th} - v_r)CV_0^2}. \tag{14}$$

We briefly review the behavior of rate and CV as functions of μ and D and then show that rate and CV uniquely fix the system's parameters.

A. Rate and CV and their contour lines in the (D, μ) plane for the PIF

The rate and CV are shown in Figs. 3(a) and 3(b) as functions of the parameters μ and D. The rate is a linear function of μ and, remarkably, does not display any dependence on D. This is a unique property of the PIF model. The CV depends linearly on $\sqrt{D/\mu}$, and can therefore attain values in the whole range $0 < CV < \infty$.

Fig. 3(c) shows contour lines for different rates and CVs, which are for both measures just straight lines. Generally, the variability of the PIF's spike train increases by decreasing the mean input and increasing the noise intensity, which is quite intuitive.

B. Uniqueness of the model parameters for a given rate and CV for the PIF

In the fairly simple case of the PIF, Eq. (13) can be readily inverted to yield μ and D as a function of rate and CV:

$$\mu = r(v_{th} - v_r), \tag{15}$$

$$D = \frac{r(v_{th} - v_r)^2 CV^2}{2}. \tag{16}$$

Eqs. (15) and (16) define a mapping $(r, CV) \mapsto (D, \mu)$, implying that for any pair (r, CV) there exists one and only one pair (D, μ).
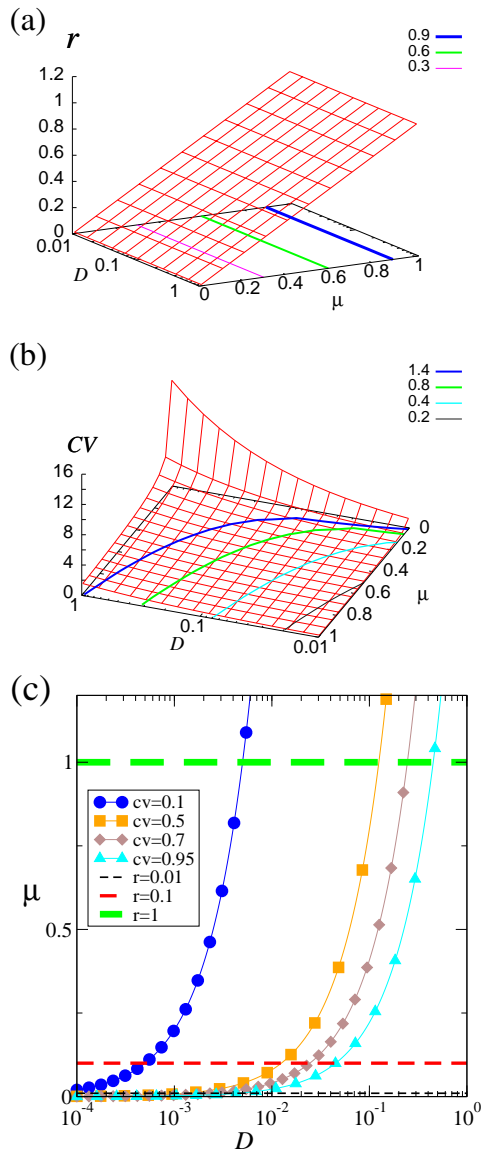
FIG. 3: Rate (a) and CV (b) as a function of the parameters μ and D for the perfect integrate-and-fire model. Contour lines for constant rate (a, c) and CV (b, c) as indicated. For illustration, the curves $r = 0.01, 0.1,$ and 1 in (c) correspond to the physiologically relevant rates 1,10, and 100 Hz, respectively, under the assumption that the membrane time constant in Eq. (1) has the typical value $\tau = 10$ ms.

IV. LEAKY INTEGRATE-AND-FIRE NEURON

For the LIF, the mean and variance of the ISIs are [1, 22, 27]:

$$\langle T \rangle = \sqrt{\pi} \int_a^b dy e^{y^2} \ \mathrm{erfc}(y), \tag{17}$$

$$\langle \Delta T^2 \rangle = 2\pi \int_a^b dz e^{z^2} \int_z^\infty dy e^{y^2} \mathrm{erfc}^2(y), \tag{18}$$

where

$$a = (\mu - v_{th})/\sqrt{2D} \text{ and } b = (\mu - v_r)/\sqrt{2D}. \tag{19}$$

From these expressions and the general relations Eq. (10) and (11), one can derive the differential equations that govern the contour lines as follows:

$$\frac{d\mu_r}{dD} = \frac{b-a}{v_{th}-v_r}\left(\frac{be^{b^2}\operatorname{erfc}(b) - ae^{a^2}\operatorname{erfc}(a)}{e^{b^2}\operatorname{erfc}(b) - e^{a^2}\operatorname{erfc}(a)}\right), \tag{20}$$

$$\frac{d\mu_{CV}}{dD} = \left(\frac{b-a}{v_{th}-v_r}\right)\left[a\left(1-\mathbb{F}(a,b)\right)^{-1} + b\left(1-\frac{1}{\mathbb{F}(a,b)}\right)^{-1}\right], \tag{21}$$

$$\mathbb{F}(a,b) = \frac{\int_a^b dx e^{x^2}\operatorname{erfc}(x)e^{b^2}\int_b^\infty dy e^{y^2}\operatorname{erfc}^2(y) - 2\int_a^b dz e^{z^2}\int_z^\infty dy e^{y^2}\operatorname{erfc}^2(y)e^{b^2}\operatorname{erfc}(b)}{\int_a^b dx e^{x^2}\operatorname{erfc}(x)e^{a^2}\int_a^\infty dy e^{y^2}\operatorname{erfc}^2(y) - 2\int_a^b dz e^{z^2}\int_z^\infty dy e^{y^2}\operatorname{erfc}^2(y)e^{a^2}\operatorname{erfc}(a)}, \tag{22}$$

$$\frac{dD_{CV}}{d\mu} = \left[\frac{d\mu_{CV}}{dD}\right]^{-1}. \tag{23}$$

We will first recall some properties of rate and CV most but not all of which have been already discussed elsewhere [27, 28].

A. Rate and CV and their contour lines in the (D,μ) plane for the LIF

Rate and CV as functions of μ and D are shown in Fig. 4. As seen in Fig. 4(a), the rate is an increasing function of μ for fixed D and an increasing function of D for fixed μ. In the zero-noise limit, the rate is zero for $\mu < v_{th}$ and increases logarithmically with μ for μ larger than but close to v_{th}.

The behavior of the CV is much richer (see Fig. 4(b)). In particular, the LIF model displays *coherence resonance* (CR) [27, 28]: for fixed $\mu < v_{th}$, the CV exhibits a minimum at a finite value of D. Coherence resonance thus corresponds to the phenomenon by which noise has the counter-intuitive effect of increasing the regularity of the spike train. For the LIF, a pronounced CR is observed for a mean input μ close to but smaller than the threshold.

The CV for the LIF can exceed unity. Loosely speaking such a regime corresponds to a firing activity more irregular than in the Poissonian regime ($CV = 1$). This high variability is associated to short ISIs occurring relatively frequently, but long ISIs being also likely. When $\mu < 0$, a simple interpretation can be made in terms of the Brownian particle in a parabolic potential. As shown in Fig. 1(f), in this case both v_r and v_{th} are larger than the value of v at which the potential attains its minimum. The short ISIs then correspond to the cases when the particle heads directly from v_r to v_{th}, while the long ones correspond to the particle first going to the minimum of the potential and then performing its excursion to v_{th}.

Independently of D, if $\mu \to -\infty$ the firing becomes Poissonian ($CV = 1$). In the opposite limit of $\mu \to \infty$, the firing is perfectly regular ($CV = 0$). At least for large noise intensity, the CV exceeds unity, as discussed above. Therefore, for fixed noise sufficiently strong we observe a maximum of the CV with respect to μ [32]. This is an interesting feature of the LIF model which to our knowledge has not been described so far.

As also shown in Fig. 4(b), the contour lines for the CV display non-monotonicities with respect to both parameters. The contour lines at which the CV is smaller than 1 display non-monotonic behavior with respect to D, whereas the ones corresponding to CV larger than 1 are non-monotonic functions of μ (see, for instance, the contour line $CV = 1.1$). Fig. 4(c) shows contour lines for rate and CV in a range of physiological interest.

We also observe that, as shown in Fig. 4(d), the contour lines of rate and CV become almost parallel in the region of small D and $\mu < v_{th}$ (see especially contour lines $r = 0.01$ and $CV = 0.95$). Thus, as the firing regime approaches the Poissonian limit, the actual determination of the intersections of the contour lines becomes a practically more difficult task. Also it becomes less clear whether there is only intersection point or not. In view of this particular (numerical) uncertainty, but also in view of the nonmonotonic behavior of the contour lines μ_{CV} as functions of D (for $\mu < v_{th}$) and μ (for strong noise), it is desirable to gain certainty about whether rate and CV uniquely determine D and μ in the LIF model.

B. Uniqueness of the model parameters for a given rate and CV for the LIF

Our strategy to show that the model parameters are uniquely determined for a given rate and CV comprises two steps. First, we show that each contour line for the rate is unique. Second, we show that the CV is a monotonic function along any rate contour line. The second step can be simplified by noting that the CV is the ratio between the square root of the *variance* $\sigma^2 = \langle\Delta T^2\rangle$ and the mean $\langle T\rangle$. Since the mean is invariant in any contour line for the rate, it suffices to show that the σ^2 is a monotonic function along any such contour line. In other words, it suffices to show that the directional derivative of σ^2 along the tangent of the contour line for the rate is strictly positive [33].
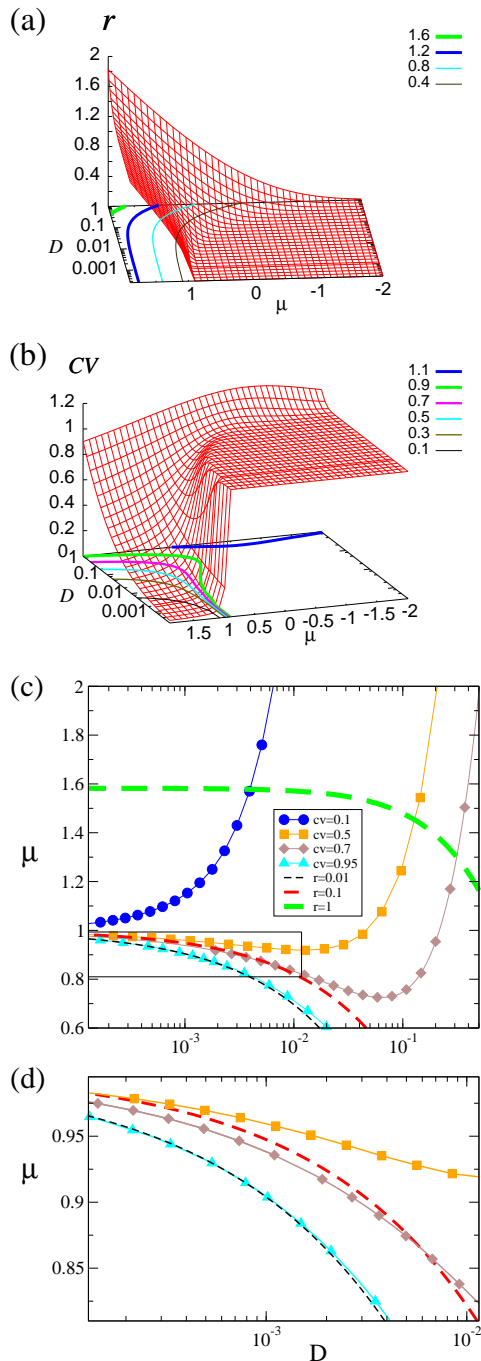
FIG. 4: Rate (a) and CV (b) as a function of the parameters μ and D for the leaky integrate-and-fire model. Contour lines for constant rate (a, c) and CV (b, c) as indicated. The rectangular region in (c) is magnified in (d).

1. Uniqueness of contour lines for the rate

Let us prove that the contour line for a specific value of the rate $r(D, \mu) = r_0$ is one single connected curve. The proof comprises three steps: First, for any point $(D, \mu) \in \mathbb{R}^+ \times \mathbb{R}$ we can locally construct a contour line $r(D, \mu) = r_0$ parametrized by $\mu_{r_0}(D)$ such that $r(D, \mu_{r_0}(D)) = r_0$. This is possible by virtue of the implicit function theorem since, as shown in Appendix A, $\partial r / \partial \mu > 0$ for all $(D, \mu) \in \mathbb{R}^+ \times \mathbb{R}$. Of course, the specific value of the rate, r_0, will depend on the point (D, μ). Second, we can extend $\mu_{r_0}(D)$ to the whole domain $D \in \mathbb{R}^+$ by connecting neighborhoods of this domain. This could be made impossible if $\mu_{r_0}(D)$ diverges at finite D. We rule this possibility out by noting that it is not consistent with the limit values of the rate at $\mu = \pm\infty$. Indeed, as we show in Appendix A, the limit of the

rate is zero (for $\mu \to -\infty$) or ∞ (for $\mu \to \infty$), values which are not attained by the rate at positive D and finite μ. Hence no contour line starting within the domain can approach the boundary $\pm\infty$ at finite D and thus there cannot be a divergence of the contour line at finite D — $\mu_{r_0}(D)$ will describe a single connected line for the whole domain $D \in \mathbb{R}^+$. Third, we show that any point at which $r = r_0$ must necessarily belong to the graph of $\mu_{r_0}(D)$. In fact, if a point (D^*, μ^*) not belonging to the graph of $\mu_{r_0}(D)$ exists such that $r(D^*, \mu^*) = r_0$, then the condition $\partial r/\partial \mu > 0$ must necessarily be violated along the line $D = D^*$. This completes the proof that the contour lines for rate are single (connected) curves.

2. Proof that σ^2 is a monotonic function along the rate contour lines

Along a contour line of the rate, the mean ISI is fixed by definition and thus the CV can only vary due to changes in the variance σ^2. Thus if we show that the variance increases monotonicly as we move along the contour line in the direction of increasing D, we will have also shown that the CV increases monotonicly if we move along the contour line in this direction.

The monotonicity of σ^2 along the rate contour lines is expressed by

$$\nabla\sigma^2 \cdot \mathbf{v_t} > 0, \tag{24}$$

where $\mathbf{v_t}$ is a vector which is tangent to these contour lines and ∇ denotes the gradient in (D, μ) space. In order to show that Eq. (24) holds, let us first determine $\mathbf{v_t}$. Along the rate contour lines, the differential equation Eq. (10) with $F = r$ holds true; its right hand side is needed for an expression of the tangent vector of the rate contour lines appearing in Eq. (24):

$$\mathbf{v_t} = \mathbf{e}_D + \frac{d\mu_r}{dD}\mathbf{e}_\mu \tag{25}$$

where $\mathbf{e}_D$ and $\mathbf{e}_\mu$ are the respective unit vectors. The relation to be shown, Eq.(24), thus corresponds to

$$\frac{\partial\sigma^2}{\partial D} + \frac{\partial\sigma^2}{\partial\mu}\frac{d\mu_r}{dD} > 0. \tag{26}$$

It is much simpler to express the derivatives on the left hand side of Eq.(26) in terms of coordinates a and b rather than D and μ. Using Eqs. (18) and (19), we obtain

$$\frac{\partial\sigma^2}{\partial D} = \frac{2\pi(b-a)^2}{(v_{th}-v_r)^2}\left(-be^{b^2}\int_b^\infty dy e^{y^2}\mathrm{erfc}^2(y) + ae^{a^2}\int_a^\infty dy e^{y^2}\mathrm{erfc}^2(y)\right) \tag{27}$$

and

$$\frac{\partial\sigma^2}{\partial\mu} = \frac{2\pi(b-a)}{v_{th}-v_r}\left(e^{b^2}\int_b^\infty dy e^{y^2}\mathrm{erfc}^2(y) - e^{a^2}\int_a^\infty dy e^{y^2}\mathrm{erfc}^2(y)\right). \tag{28}$$

Inserting Eqs. (20, 27-28) into Eq.(26), and performing straightforward algebra, we write the latter as:

$$\frac{2\pi(b-a)^3 e^{a^2+b^2}}{(v_{th}-v_r)^2(e^{a^2}\mathrm{erfc}(a)-e^{b^2}\mathrm{erfc}(b))}\left(\mathrm{erfc}(b)\int_a^\infty dy e^{y^2}\mathrm{erfc}^2(y) - \mathrm{erfc}(a)\int_b^\infty dy e^{y^2}\mathrm{erfc}^2(y)\right) > 0. \tag{29}$$

This is the inequality to be shown. The prefactor on the left hand side is positive since $a < b$ and by virtue of Eq. (A1) of the Appendix. Therefore it suffices to show that

$$\mathrm{erfc}(b)\int_a^\infty dy e^{y^2}\mathrm{erfc}^2(y) - \mathrm{erfc}(a)\int_b^\infty dy e^{y^2}\mathrm{erfc}^2(y) > 0. \tag{30}$$

This is equivalent to proving that the function

$$f(x) = \frac{\int_x^\infty dy e^{y^2}\mathrm{erfc}^2(y)}{\mathrm{erfc}(x)}$$

is a monotonicly decreasing function of x. For this to hold true, the derivative of $f(x)$ should be negative for all x, i.e.

$$\frac{df}{dx} = \frac{2}{\sqrt{\pi}\mathrm{erfc}^2(x)}\int_x^\infty dy \left(e^{y^2-x^2}\mathrm{erfc}^2(y) - e^{x^2-y^2}\mathrm{erfc}^2(x)\right) < 0. \tag{31}$$

The prefactor is positive and the integrand is strictly negative for all $y > x$. The latter can be seen by multiplying the integrand by $e^{x^2+y^2}$ from which we obtain $(e^{y^2}\mathrm{erfc}(y))^2 - (e^{x^2}\mathrm{erfc}(x))^2$, which is negative as shown in the Appendix (see Eq.(A1)). The proof of Eq. (24) is therefore completed.

C. Determination of input parameters from rate and CV for the LIF

The input parameters associated to a given rate r_0 and coefficient of variation CV_0 can be obtained by means of a simple numerical algorithm, provided that the internal parameters (τ, v_{th}, and v_r) are already known.

The first step is to find a point in the $D - \mu$ space at which the rate is equal to r_0 (as measured in units of τ^{-1}). This can be most easily accomplished with the use of the property $\partial r / \partial \mu > 0$ (see the Appendix). More specifically, one starts by calculating the rate at an arbitrary point (D_0, μ_0) and then defining the next candidate point as $(D_0, \mu_0 + \Delta\mu)$, where $\Delta\mu$ is positive (negative) if the rate at (D_0, μ_0) is smaller (larger) than r_0. This is done until one crosses the contour line $r = r_0$, at which point $\Delta\mu$ should be multiplied by some factor in the interval $(-1, 0)$. This procedure can be done iteratively until one obtains a point (D^*, μ^*) at which the rate is as close to r_0 as desired.

The second step is to move along the contour line $r = r_0$ until the point at which $CV = CV_0$ is reached. This can be done by following a procedure analogous to the first step, since the directional derivative $\nabla\sigma^2 \cdot \mathbf{v_t}$ is strictly positive (see Eq. (24)). One thus integrates Eq. (20) in the direction of positive (negative) D if $CV(D^*, \mu^*)$ is smaller (larger) than CV_0. After integer multiples of n_0 times the integration step ΔD, one checks whether the contour line $CV = CV_0$ has been crossed. If the crossing has occurred, one inverts the direction of integration of Eq. (20) and multiplies n_0 by some factor in the interval $(-1, 0)$. This is done iteratively until one obtains a point (D, μ) at which the CV is sufficiently close to CV_0.

This naive algorithm already permits a fast determination of D and μ associated to a given rate and CV.

V. QUADRATIC INTEGRATE-AND-FIRE NEURON

For the QIF, one has [13]:

$$\langle T \rangle = \left(\frac{9}{D}\right)^{1/3} I(\alpha), \quad I(\alpha) = \int\limits_{-\infty}^{\infty} dx \, e^{-\alpha x - x^3} \int\limits_{-\infty}^{x} dy \, e^{\alpha y + y^3}, \tag{32}$$

$$\langle \Delta T^2 \rangle = \left(\frac{9}{D}\right)^{2/3} \int_{-\infty}^{\infty} dx e^{-\alpha x - x^3} \int_{x}^{\infty} dy e^{-\alpha y - y^3} \left[\int_{-\infty}^{x} dz e^{\alpha z + z^3}\right]^2, \tag{33}$$

$$\alpha = \left(\frac{3}{D^2}\right)^{1/3} \mu. \tag{34}$$

For this model, the following scaling relations [13] facilitate the determination of the contour lines in parameter space for rate and CV:

$$r(\mu, D) = \sqrt{|\mu|} r(\frac{\mu}{|\mu|}, |\mu|^{-3/2} D), \tag{35}$$

$$CV(\mu, D) = CV(\frac{\mu}{|\mu|}, |\mu|^{-3/2} D). \tag{36}$$

The scaling relation Eq. (36), together with the monotonicity of the CV for $\mu = \pm 1$ (see [13]), implies that (for $\mu = \pm 1$) a certain value of the CV (say, CV_0) determines uniquely the noise intensity D which we call $\bar{D}$. With this observation, the contour lines for the CV for arbitrary μ can be explicitly written:

$$\mu_{cv}(D) = \frac{\mu}{|\mu|} \left(\frac{D}{\bar{D}}\right)^{2/3}. \tag{37}$$

For the rate, $\bar{D}$ can be regarded as a parameter of the curve $\mu_r(D)$: from the above definition of $\bar{D}$ and from the scaling relation for the rate Eq. (35) we can infer that

$$\mu(\bar{D}) = \frac{\mu}{|\mu|} \left(\frac{r_0}{r(\frac{\mu}{|\mu|}, \bar{D})}\right)^2, \quad D(\bar{D}) = \bar{D} \left(\frac{r_0}{r(\frac{\mu}{|\mu|}, \bar{D})}\right)^3 \tag{38}$$

describe all the points on the curve $\mu_r(D)$ which we get by varying $\bar{D}$.

We will now recall some properties of rate and CV which have been already discussed in Ref. [13].

A.   Rate and CV and their contour lines in the (D, μ) plane for the QIF

Rate and CV as a function of μ and D are shown in Fig. 5. The behavior of the rate is similar to the case of the LIF. Here again it is a monotonicly increasing function of μ for fixed D and monotonicly increasing function of D for fixed μ. A noticeable difference arises in the zero-noise limit and close to the bifurcation at $\mu = 0$: the rate for the QIF is also strictly zero if $\mu \leq 0$ but, differently from what is observed for the LIF, it increases proportionally to the square root of μ for small positive μ.

In clear contrast with the LIF and PIF, the CV for the QIF is bounded in the interval $0 < CV < 1$. Moreover, here the CV is a strictly monotonic function of both D and μ. For fixed D, it decreases with increasing μ and, for fixed positive (negative) μ, it increases (decreases) with increasing D. Therefore, coherence resonance does not occur for this model.

Fig. 5c shows some contour lines for rate and CV in the physiologically relevant region of the parameter space. We stress out that for the QIF the contour lines of the CV are monotonic functions of both D and μ.

B.   Uniqueness of the model parameters for a given rate and CV for the QIF

We will consider as given that the $CV(1, \bar{D})$ ($CV(-1, \bar{D})$) is a monotonically increasing (decreasing) function of $\bar{D}$; this was demonstrated in [13] by limit cases and by numerical evaluation of the integrals. From these properties we can conclude: for negative (positive) μ, decreasing (increasing) the CV from 1 (0) to $3^{-1/2}$, the parameter $\bar{D}$ changes monotonically from 0 to infinity implying that each CV between 0 and 1 has one unique contour line parametrized by the sign of μ and the value of $\bar{D}$ (see Eq.(37)). The value $\mu = 0$ is a special case where the CV attains exactly the value at the boundary between both regimes $\mu < 0$, $\mu > 0$, namely, CV=$3^{-1/2}$ [29].

If we can show that the rate or equivalently the mean ISI changes monotonically along the contour lines of the CV, then there is at most one intersection for a given pair of CV and rate and thus the mapping of rate and CV to μ and D is unique. Note that although our argument is similar to the one used for the LIF, we will consider the change in the mean ISI along the curve of constant CV and not the change in CV (or variance) along a curve of constant rate as we did for the LIF.

The directional derivative of the mean ISI along the CV contour line reads

$$\nabla \langle T \rangle \cdot \mathbf{v_t} = \frac{\partial \langle T \rangle}{\partial D} + \frac{\partial \langle T \rangle}{\partial \mu} \frac{d\mu_{CV}}{dD} \tag{39}$$

From Eq. (37), we obtain:

$$\frac{d\mu_{cv}}{dD} = \frac{\mu}{|\mu|} \frac{2}{3} D^{-1/3} \bar{D}^{-2/3}, \tag{40}$$

Using this expression and Eqs. (32) and (34), one can rewrite the directional derivative as follows:

$$\nabla \langle T \rangle \cdot \mathbf{v_t} = -\frac{1}{3D} \langle T \rangle - \frac{2}{D^2} \frac{\partial I(\alpha)}{\partial \alpha} \left[\mu - \frac{\mu}{|\mu|} \left(\frac{D}{\bar{\bar{D}}} \right)^{2/3} \right] \tag{41}$$

The expression in the brackets vanishes by definition since it equals $\mu - \mu_{CV}$. Hence we find that the last term is truly zero and thus the directional derivative of the mean ISI along the contour lines of the CV is negative throughout the (μ, D) plane

$$\nabla \langle T \rangle \cdot \mathbf{v_t} = -\frac{1}{3D} \langle T \rangle < 0 \tag{42}$$

We have thus shown that (i) for each CV between 0 and 1 there exists exactly one contour line and (ii) the mean ISI decreases always as we go along these contour lines in direction of increasing noise intensity. Hence, each mean ISI is at most represented once on a contour line of the CV and thus for each pair of rate and CV values there is at most one pair (μ, D).

C.   Determination of input parameters from rate and CV for the QIF

The parameters D and μ can be obtained numerically from a given rate r_0 and $CV = CV_0$ for the QIF provided that the membrane time constant is known. This is an advantage with respect to the LIF, for which the threshold and reset potentials are also needed.

The first and more cumbersome step is the numerical determination of the four curves $r(\pm 1, D)$, $CV(\pm 1, D)$. These curves can be determined directly from Eqs. 32 and 33.

The second step is the determination of the contour lines $r = r_0$ and $CV = CV_0$, where r_0 is measured in units of τ^{-1}. The first can be directly obtained from the parametric equations Eq. (38), where $\bar{D}$ is the free parameter. The second can be straightforwardly determined from Eq. (37), where $\bar{D}$ is now the noise intensity such that $CV(\frac{\mu}{|\mu|}, \bar{D}) = CV_0$.
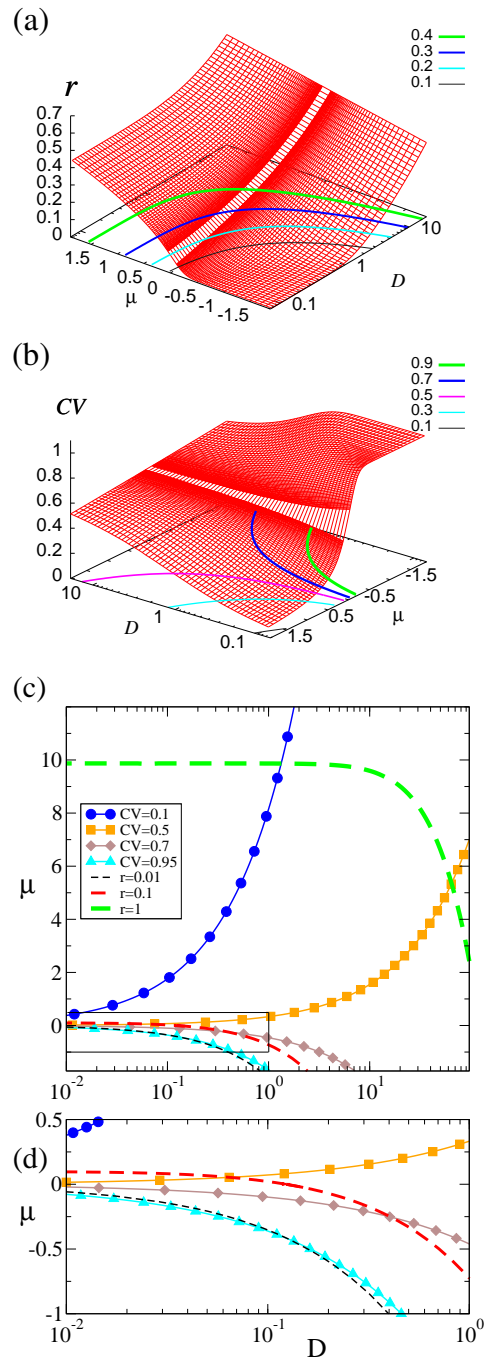
FIG. 5: Rate (a) and CV (b) as a function of the parameters μ and D for the quadratic integrate-and-fire model. Contour lines for constant rate (a, c) and CV (b, c) as indicated. The rectangular region in (c) is magnified in (d). The more sparse grid in the region close to $\mu = 0$ in (a, b) is due to the way we generated the points and does not reflect any property of the surfaces $r(D, \mu)$ and $CV(D, \mu)$.

VI. CONCLUSIONS

To summarize, we have reviewed the behavior of rate and CV as functions of the input parameters for three different IF models. As the central result of our paper, we have shown that these statistics uniquely determine the input parameters for the models studied. This sets a framework for systematic comparison of these models: they can be fairly compared when their parameters are tuned so as to yield the same rate and CV. Reports on these comparisons will be published elsewhere. A possibly useful byproduct of our study comprises simple formulas (PIF) or algorithms (LIF and QIF) for a fast determination of the parameters D and μ associated to a given rate and CV,

which may be of instrumental value for experimentalists and modelers.

It is tempting to consider the general IF model with white noise input: do rate and CV determine the input parameters for an arbitrary nonlinear function $f_{\text{model}}(v)$ or equivalently for an arbitrary nonlinear potential $U(v)$? Unfortunately, so far no general procedure to show the uniqueness of input parameters is known. What we showed in this paper relied on model-specific properties of the ISI moments for the PIF, LIF, and QIF. Approaches to the uniqueness problem based on the general formulas for the moments of the first-passage-time could lead to conditions on the potential $U(v)$ and the reset and threshold values of the IF model; however, we have not made any progress in this direction yet. We note that it may still be worth the effort to prove the uniqueness of parameter values for a given rate and CV for other specific neuron models of the IF type. One such a case is the exponential IF model [5], which has been successfully used to describe pyramidal neurons activity [15].

Another and more complicated open problem is to check whether the uniqueness of parameters also holds for more complex models, such as those taking adaptation, reversal potentials, subthreshold oscillations, or relative refractory effects into account. Finally, the questions treated here may be worth to be addressed as well in cases where the neurons are subjected to colored noise, either caused by a finite synaptic time constant [30] or by temporal correlations in the pre-synaptic input [31].

APPENDIX A: SOME PROPERTIES OF THE RATE IN THE LIF MODEL

We start by proving that the function $g(x) = \exp(x^2)\text{erfc}(x)$ is monotonicly decreasing for all $x \in \mathbb{R}$. Writing explicitely $\text{erfc}(x) = 2/\sqrt{\pi} \int_x^\infty dt \exp(-t^2)$ and performing the changes of variables $s' = t - x$ and $s'' = t - y$, we obtain

$$g(x) - g(y) = \frac{2}{\sqrt{\pi}} \left(\int_0^\infty ds' e^{-s'^2 - 2xs'} - \int_0^\infty ds'' e^{-s''^2 - 2ys''} \right) = \frac{2}{\sqrt{\pi}} \int_0^\infty ds e^{-s^2} (e^{-2xs} - e^{-2ys}) > 0 \text{ if } x < y, \quad \text{(A1)}$$

since $s \geq 0$. Therefore $g(x)$ is indeed a monotonicly decreasing function.

Second, we observe that

$$\lim_{x \to \infty} \text{erfc}(x)e^{x^2} = 0. \quad \text{(A2)}$$

In fact, writing again the explicit formula for erfc and applying L'Hospital's rule, we obtain

$$\lim_{x \to \infty} \text{erfc}(x)e^{x^2} = \lim_{x \to \infty} \frac{2}{\sqrt{\pi}} \frac{\int_x^\infty dt \exp(-t^2)}{e^{-x^2}} = \lim_{x \to \infty} \frac{2}{\sqrt{\pi}} \frac{-e^{-x^2}}{-2xe^{-x^2}} = 0. \quad \text{(A3)}$$

Now let us prove that for the LIF one has

$$\partial r/\partial \mu > 0. \quad \text{(A4)}$$

Eqs. (17) and (19) imply that

$$\partial \langle T \rangle / \partial \mu = \frac{1}{\sqrt{2D}} \left(\partial \langle T \rangle / \partial a + \partial \langle T \rangle / \partial b \right). \quad \text{(A5)}$$

Now,

$$\partial \langle T \rangle / \partial a + \partial \langle T \rangle / \partial b = \sqrt{\pi}(e^{b^2} \text{ erfc}(b) - e^{a^2} \text{ erfc}(a)). \quad \text{(A6)}$$

We thus obtain:

$$\frac{\partial \langle T \rangle}{\partial \mu} = \sqrt{\frac{\pi}{2D}}(e^{b^2} \text{ erfc}(b) - e^{a^2} \text{ erfc}(a)) < 0, \quad \text{(A7)}$$

since $a < b$ and by virtue of Eq. (A1). Eq. (A4) is therefore proved.

Next let us prove that

$$\lim_{\mu \to \infty} r = \lim_{\mu \to \infty} \frac{1}{\langle T \rangle} = \infty \quad \text{and} \quad \lim_{\mu \to -\infty} r = \lim_{\mu \to -\infty} \frac{1}{\langle T \rangle} = 0. \quad \text{(A8)}$$

for which it suffices to show that the mean interval approaches zero or infinity as μ goes to plus or minus infinity, respectively. The integrand in the integral expression for the mean interval Eq. (17) is a monotonically decreasing function as shown above in Eq. (A1); with this property we can estimate

$$\sqrt{\pi}(b - a)\text{erfc}(b)e^{b^2} \leq \langle T \rangle \leq \sqrt{\pi}(b - a)\text{erfc}(a)e^{a^2} \quad \text{(A9)}$$

which is equivalent to

$$\text{erfc}(b)e^{b^2} \leq \sqrt{\frac{2D}{\pi}} \frac{\langle T \rangle}{v_{th} - v_r} \leq \text{erfc}(a)e^{a^2} \tag{A10}$$

For $\mu \to \infty$ both $a, b \to \infty$ and the functions on the left and right hand sides go to zero as shown in Eq. (A3). Thus, we obtain in this limit what proves the first of our limit cases in Eq. (A8):

$$\lim_{\mu \to \infty} \langle T \rangle = 0. \tag{A11}$$

In the opposite limit of $\mu \to -\infty$, both $a, b \to -\infty$; the complementary error function attains a finite value in this limit ($\lim_{x \to -\infty} \text{erfc}(x) = 2$) and the exponential functions then yield a divergence of both sides yielding

$$\lim_{\mu \to -\infty} \langle T \rangle = \infty. \tag{A12}$$

which proves the second of the asserted limit cases in Eq. (A8).

Acknowledgments

[1] H. C. Tuckwell, *Introduction to Theoretical Neurobiology* (Cambridge University Press, Cambridge, 1988).
[2] A. N. Burkitt, Biol. Cyber. **95**, 1 (2006).
[3] E. M. Izhikevich, Neural Networks **14**, 883 (2001).
[4] E. Salinas and T. J. Sejnowski, J. Neurosci. **20**, 6193 (2000).
[5] N. Fourcaud-Trocmé, D. Hansel, C. van Vreeswijk, and N. Brunel, J. Neurosci. **23**, 11628 (2003).
[6] H. C. Tuckwell, Biol. Cyb. **30**, 115 (1978).
[7] B. Lindner and A. Longtin, J. Theo. Biol. **232**, 505 (2005).
[8] G. L. Gerstein and B. Mandelbrot, Biophys. J. **4**, 41 (1964).
[9] R. B. Stein, Biophys. J. **5**, 173 (1965).
[10] R. B. Stein, Biophys. J. **7**, 37 (1967).
[11] P. Johannesma, in *Neural Networks*, edited by E. Caianiello (Springer, Berlin, 1967), p. 116.
[12] B. S. Gutkin and G. B. Ermentrout, Neural Comp. **10**, 1047 (1998).
[13] B. Lindner, A. Longtin, and A. Bulsara, Neural. Comp. **15**, 1761 (2003).
[14] P. Lánský and S. Ditlevsen, Biol. Cybern. (2008).
[15] L. Badel, S. Lefort, R. Brette, C. C. H. Petersen, W. Gerstner, and M. J. E. Richardson, J. Neurophysiol. **99**, 656 (2008).
[16] H. C. Tuckwell and W. Richter, J. Theor. Biol. **71**, 167 (1978).
[17] J. Inoue, S. Sato, and L. M. Ricciardi, Biol. Cybern. **73**, 209 (1995).
[18] A. Rauch, G. L. Camera, H.-R. Lüscher, W. Senn, and S. Fusi, J. Neurophysiol. **90**, 1598 (2003).
[19] G. L. Camera, A. Rauch, H.-R. Lüscher, W. Senn, and S. Fusi, Neural Computation **16**, 2101 (2004).
[20] G. B. Ermentrout, Neural. Comp. **8**, 979 (1996).
[21] L. Pontryagin, A. Andronov, and A. Witt, Zh. Eksp. Teor. Fiz. **3**, 172 (1933), reprinted in *Noise in Nonlinear Dynamical Systems*, 1989, ed. by F. Moss and P. V. E. McClintock (Cambridge University Press, Cambridge), Vol. 1, p. 329.
[22] L. M. Ricciardi, *Diffusion Processes and Related Topics on Biology* (Springer-Verlag, Berlin, 1977).
[23] A. V. Holden, *Models of the Stochastic Activity of Neurones* (Springer-Verlag, Berlin, 1976).
[24] P. Colet, M. S. Miguel, J. Casademunt, and J. M. Sancho, Phys. Rev. A **39**, 149 (1989).
[25] A. Bulsara, S. B. Lowen, and C. D. Rees, Phys. Rev. E **49**, 4989 (1994).
[26] A. Bulsara, T. C. Elston, C. R. Doering, S. B. Lowen, and K. Lindenberg, Phys. Rev. E **53**, 3958 (1996).
[27] B. Lindner, L. Schimansky-Geier, and A. Longtin, Phys. Rev. E **66**, 031916 (2002).
[28] K. Pakdaman, S. Tanabe, and T. Shimokawa, Neural Networks **14**, 895 (2001).
[29] D. Sigeti and W. Horsthemke, J. Stat. Phys. **54**, 1217 (1989).
[30] N. Brunel and S. Sergi, J. Theor. Biol. **195**, 87 (1998).
[31] B. Lindner, Phys. Rev. E **69**, 022901 (2004).
[32] The existence of this maximum was pointed out to the authors by Tilo Schwalger, *Max-Planck-Institut für Physik Komplexer Systeme (Dresden)*.
[33] The basic idea for this step in the proof is due to Dr. Jochen Bröcker, *Max-Planck-Institut für Physik Komplexer Systeme (Dresden)*.